

A MODE BASED APPROACH FOR CHARACTERIZING RF PROPAGATION IN CONDUITS

I. L. Howitt and M. S. Khan

Department of Electrical and Computer Engineering
The University of North Carolina at Charlotte
Charlotte, NC 28223, USA

Abstract—We propose a mode based approach for developing a parametric model to characterize RF propagation in conduits. The model considers a conduit as a lossy waveguide and defines the total received power as the sum of powers excited in propagating modes. The model's parameters are estimated from both the physical properties of the conduit material and an empirical data set. Underground conduits have significant value as wireless communication channels for condition based monitoring within the conduit. An enabler for this wireless sensor network application is based on characterizing the expected coverage range of wireless transceivers operating in the 2.4 GHz ISM band. Previous studies on modeling RF propagation in underground conduits have focused on conduits with diameters larger than 1.05 m. This motivated our measurement campaign to collect empirical data from underground conduits with varying diameters from 0.30 m to 1.37 m. The empirical data is used to predict the mode coupled powers which are model parameters that are analytically intractable. We observe that the proposed model provides a good estimate of received power in terms of contribution from dominant propagating modes.

1. INTRODUCTION

Radio frequency (RF) signal propagation in confined underground ducts has been an important area of research driven primarily by rapid developments in wireless communication technologies. Early development was motivated by the cellular telephony industry based on the need to understand cellular coverage within transportation tunnels. More recently, with the advent of wireless sensor networks (WSN), there is a need to extend the understanding to underground conduits such as storm and waste water pipes.

Corresponding author: M. S. Khan (mkhan8@uncc.edu).

RF propagation characteristics, specifically the expected coverage range, are an enabler for wireless communication applications. Traditionally, RF propagation measurements are made within the application environment to obtain this insight. Analytical models derived based on the empirical data are useful to interpolate over the bounds of the measured data. Obtaining a robust empirical data set required to derive these analytical models is not always feasible. This was the dilemma we faced when evaluating limited data sets based on our measurement campaign to characterize RF propagation within storm drain pipes. By exploiting the physical properties of buried conduits in conjunction with our limited measurement data set we propose a general and novel approach for modeling RF propagation characteristics in underground conduits.

In order to develop the generalized modeling approach, we start with an established physics-based analytical model which we use to characterize the RF propagation in storm drain pipes (SDPs). The model considers the SDP as a leaky waveguide and defines the total received power at a distance from the transmitter as the sum of powers excited in propagating modes. The *Mode Based Model* (MBM) establishes an analytical relationship between received power versus distance based on the physical properties of the conduit. In order to complete the RF propagation analysis, the MBM is used with the empirical measurement data to estimate the power coupled into each mode (mode coupled power). Evaluating the mode coupled power is, in general, analytically intractable and therefore needs to be estimated based on the empirical data. As presented in the paper, the MBM provides a general framework with which RF propagation characteristics within a conduit can be estimated based on a limited data set.

The principal motivation is to characterize the expected coverage range corresponding to typical wireless transceivers operating in the 2.4 GHz ISM band, especially the Wireless Sensor Networks (WSN) deployed for condition monitoring of underground pipes. Based on this goal, the MBM needs to reliably estimate received power characteristics over an approximate 110 dB dynamic range. This requirement is based on typical wireless transceivers in the 2.4 GHz band with 0 dBm to 15 dBm transmit power and nominal -95 dBm to -105 dBm receiver sensitivity thresholds.

Historical research conducted on communication through underground structures focused on understanding radio frequency propagation in coal mines, railroad, auto, subway tunnels and heating, ventilation and air conditioning (HVAC) ducts [1–5]. In [6] the authors have proposed a Multimode model based on geometrical Optical (GO) ap-

proach to analyze the electromagnetic field distribution inside the tunnel waveguide. In [7], an Alternate Direction Implicit (ADI) method using a Parabolic Equation (PE) is employed to model radio wave propagation in real tunnels at large distances where lower order modes are dominant. More recently, a SewerSnort system has been proposed in [8] that uses Wireless Sensor Networks (WSN) for in-sewer gas monitoring. The SewerSnort system requires characterization of wireless channel in the conduit for Received Signal Strength Indicator (RSSI) based sensor localization.

The closest parallels to the present study are two investigations into using hand-held RF devices within relatively large diameter underground conduits. In [9], RF propagation was evaluated for maintenance worker communication while inspecting, repairing and cleaning water reclamation tunnels. In [10], 1.06 m diameter sewer-lines were investigated for use as secure communication channels during military operations in urban terrain.

The reports in [9, 10], however, do not address the scope of issues associated with using WSNs for condition based monitoring within underground conduits. A specific WSN application under investigation addresses sanitary sewer overflows (SSO) which are a major concern for municipal utility operators due to their resulting environmental impact. A condition based monitoring system for detecting the onset of SSOs as defined in [11] uses WSNs as an integral component. Hence, there is a need to have a general evaluation of RF propagation in underground conduits.

The remainder of the paper is organized as follows. Section 2 presents the development of Mode Based Model (MBM). Section 3 evaluates the MBM applied to RF propagation within SDPs. The conclusions are presented in Section 4.

2. MODE BASED MODEL DEVELOPMENT

Various methods are available for characterizing wireless communication channels. The channel impulse response enables characterization of frequency response through classical transformation techniques, e.g., FFT. Average path loss models have also been proposed to predict the received power levels in indoor and urban area environments [12, 13]. Another common empirical approach in channel modeling involves curve fitting or determining analytical expressions through regression/interpolation to estimate model parameters based on measured data. For developing the MBM, we follow a circular leaky waveguide model for the SDP and analyze the model by taking into account the power contained in the propagating modes and their at-

tenuation coefficients [14]. The detailed approach for developing the MBM is given in the ensuing paragraphs.

We start the development using a well-established model for a leaky circular waveguide [15], where the n -th mode's attenuation coefficient, α_n , depends upon the mode's cut-off frequency. For imperfectly conducting walls [15]

$$\alpha_n = B R_s \left/ \left(\eta a \sqrt{1 - (f_c/f)^2} \right) \right. \quad (1)$$

where $B = (f_c/f)^2 + (n^2/(p'_{nm}{}^2 - n^2))$ for TE modes and $B = 1$ for TM modes; η is the magnitude of the intrinsic impedance of the waveguide wall material; R_s is the real part of the intrinsic impedance of the waveguide walls given by $R_s = \sqrt{\pi\mu f/\sigma}$, where μ is the permeability and σ is the electrical conductivity of the wall material. In (1), α_n is expressed in nepers/m. It is often more effective to express α_n in dB/m by using α [dB/m] = $20 \log_{10}(e) \times \alpha$ [nepers/m].

The relationship for attenuation coefficient in (1) was derived using perturbational method [15] and, as indicated by the author, the model is valid for waveguides having imperfectly conducting walls. The attenuation coefficient relationship given in (1) includes power dissipated in the guide walls and does not take into account power dissipation due to imperfect dielectric medium inside the guide. Modeling the SDP as a leaky waveguide assumes losses associated with the dielectric medium (air) which are negligibly small when compared to power dissipation caused by the imperfectly conducting walls.

The MBM is based on considering the modal components of the RF signal within the SDP. The power contained in a mode decays exponentially with the product of the attenuation coefficient and the distance. The total received power at a distance d from the source is the summation of the exponentially decaying modal powers [14]

$$P_R(d) = \sum_{n=1}^N P_n e^{-2\alpha_n d} \quad (2)$$

where P_n is the mode coupled power representing the power in mode n coupled into the medium from the transmit antenna.

In order to evaluate (2), $\{P_n, \alpha_n\} \forall n$ needs to be estimated. The attenuation coefficients, α_n , can be estimated based on the physical properties of the SDP using (1). P_n needs to incorporate n -th mode's coupling between the medium and antenna at both the transmit and receive antennas. Deriving analytical or numerical estimates for P_n are, in general, intractable except under specific conditions [5]. In our proposed approach for deriving the MBM, an empirical data

set $\{\{d_i, P_R(d_i)\} \forall i = 1, \dots, M\}_{Measured\ Data}$ is used for estimating P_n . The method for deriving the proposed MBM can be viewed as

$$\hat{P}_R(d) = f(d, \{P_n\} | \{\alpha_n\}) \quad (3)$$

where the attenuation coefficients, α_n , are estimated based on (1) and the optimal values of mode coupled power, $\{P_n\}^*$ are optimized based on empirical data. The optimization approach is presented in Section 3.2 following a discussion of the measurement campaign presented in Section 3.1.

3. MBM EVALUATION FOR THE SDP

3.1. Measurement Campaign

A measurement campaign was conducted at various locations in Charlotte, NC to obtain RF propagation measurements within SDPs. The details of the campaign are presented in [14, 16, 17]. The specific objectives of the measurement campaign were to characterize RF propagation over

- The 2.4 GHz ISM band,
- Variations in the SDP diameters feasible for supporting RF communications,
- Variations in SDP lengths consistent with wireless transceivers operational range,
- Variations in the transmit and receive antennas placement within the SDP pipe opening, e.g., middle versus top of the pipe.

All the objectives of the empirical measurement campaign were not fully obtained. The details of the measurement campaign are

Table 1. Summary of the SDP empirical measurement campaign.

SDP Diameter (m)	No. of Measurement Points	Max. Dist. (m)	No. of Modes at $f = 2.5$ GHz	Min. cut-off freq. (MHz)	Min. Atten. Coef. (dB/m)
0.30	5	13.0	17	577	12.63
0.46	4	23.3	40	385	3.22
0.76	5	67.3	104	231	0.70
1.07	7	28.5	196	165	0.24
1.37	3	27.4	278	128	0.11

summarized in Table 1. Principally, the goal of acquiring a data set, $\{d_i, P_R(d_i)\}$ $i = 1, \dots, M$, over the 110 dB wireless receiver dynamic range was not consistently achieved. This goal was complicated due to the lack of accessibility to SDPs. This limitation motivated the MBM approach proposed in this paper, i.e., the ability to derive the MBM based on a limited empirical data set.

From Table 1, for SDPs with pipe diameters < 0.76 m, the minimum attenuation coefficient suggests wireless transceivers would have limited transmission ranges and they are of less interest for wireless communication applications. Therefore, our study focused on the data collected for the 0.76 m and 1.07 m SDPs. Scatter plots of the empirical data collected for these SDPs are graphed in Fig. 1. The measurements are based on the Tx and Rx antennas located in the center of the SDPs.

For each $\{d_i, P_R(d_i)\}$, the received power is based on averaging over measurements taken at eleven frequencies, $\{2.4, 2.41, \dots, 2.5$ GHz $\}$. A typical frequency response is graphed in Fig. 2 for 1.07 m SDP with $d_i \approx 20$ m. As discussed in [4], the $\{2.4, 2.41, \dots, 2.5$ GHz $\}$ measurements span multiple coherence bandwidths. This is exhibited in Fig. 2 by the variation in the received power over the band. To mitigate the effects of the received power variation due to frequency dependency, the data sets used to derive the MBM are based on the average received power over the frequency band.

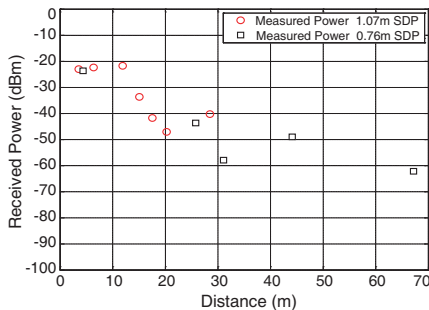


Figure 1. Scatter plot of measured power — 1.07 m and 0.76 m diameter SDPs.

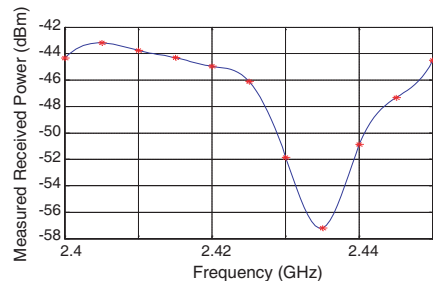


Figure 2. Received power measurements, “*”, over the 2.4 GHz ISM band within a 1.07 m SDP at ~ 20 m distance.

3.2. MBM Evaluation

As expressed in (2), the MBM can be used to estimate $P_R(d)$ given $\{P_n, \alpha_n\} \forall n$. As indicated in Section 2, the proposed method for estimating the parameters is based on (3). This approach exploits the individual mode propagation characteristics. Specifically, the cut-off frequencies of the excited modes determine their propagating or evanescent nature. The propagating modes, with cut-off frequencies closest to the operating frequency, have the highest attenuation and highest initial energy. In contrast, the lower order modes have lower coupled power; but, due to their smaller attenuation coefficients, they are dominant at greater distances. The variation in the modes contribution to the total power as a function of distance is key in devising the MBM for estimating the received power.

The general approach for deriving the MBM based on empirical data set $\{d_i, P_R(d_i)\} i = 1, \dots, M$, for an SDP with radius a is:

1. Use (1) to estimate α_n based on the SDP radius and the SDP's physical properties given by the intrinsic impedance ratio R_s/η ,
2. Use (2) in conjunction with the empirical data set to determine the optimal $\{P_n\}^*$ in the mean squared error (MSE) sense,

$$\{P_n\}^* = \arg \min_{\{P_n\}} \left\{ \sum_{i=1}^M \left(P_R(d_i) - \hat{P}_R(d_i) \right)^2 \right\} \quad (4)$$

$$\text{with } 0 \leq P_n \leq P_{\max} \forall n,$$

3. Using the solution in (4), the MBM's root mean square error (RMSE) is

$$\bar{\varepsilon} = \left\{ \frac{1}{M} \sum_{i=1}^M \left(P_R(d_i) - \hat{P}_R(d_i) \right)^2 \right\}^{1/2}. \quad (5)$$

The following three issues arise when the procedure is applied to a limited empirical data set where the number of data points is significantly less than the number of modes ($M \ll N$)

- Selecting the modes used in deriving $\{P_n, \alpha_n\}$ and to evaluate (2),
- Uncertainty associated with the SDP's physical construction which governs R_s/η ,
- Optimizing $\{P_n\}$.

Each of these issues is addressed in the following three subsections. The empirical data set used in the evaluation is from the 1.07 m SDP measurement consisting of seven measurements, $M = 7$. In this section, MBM is also compared with a standard regression modeling method. The empirical data from both the 0.76 m and 1.07 m SDPs are used in this comparison.

3.2.1. Mode Selection

The objective function, $J(\{P_n\}|\{\alpha_n\})$, underlying (4) is an ellipsoid obtained by using (2)

$$J(\{P_n\}|\{\alpha_n\}) = \sum_{i=1}^M \left(P_R(d_i) - \left[\sum_{n=1}^N C_{in} P_n \right] \right)^2 \quad (6)$$

where $C_{in} = e^{-2\alpha_n d_i}$. The objective function in (6) is a monotonically decreasing convex function, mapping $\mathfrak{R}^N \rightarrow \mathfrak{R}$. The solution space for the optimization of (6) is the intersection of $J(\cdot)$ with the N -dimensional hypercube, $\{0 \leq P_n \leq P_{\max}\}$, $n = 1, \dots, N$. The intersection between $J(\cdot)$ and the optimization constraint is also convex [18] with a unique minimum residing either within the hypercube or on its edge.

The dimensionality of the ellipsoid described by $J(\cdot)$ is based on the number of modes N . To illustrate, for the 1.07 m SDP, there are 197 modes at 2.5 GHz resulting in $J(\cdot)$ mapping $\mathfrak{R}^{197} \rightarrow \mathfrak{R}$. The modes for this SDP are comprised of 104 TE and 93 TM modes. The minimum TM attenuation coefficient is 13 dB/m, indicating that TM modes, as a whole, become evanescent over a short distance. Therefore, the coefficients C_{in} corresponding to the TM modes are relatively small, resulting in the ellipsoid collapsing or nearly collapsing to a line in the TM mode dimensions. In a similar fashion, the majority of the TE modes have relatively large attenuation coefficients. This again results in an additional dimensionality reduction in $J(\cdot)$.

Table 2 provides a rank ordered list of the modes with the ten smallest attenuation coefficients for the 1.07 m SDP. In the last three columns of the table, a comparison is provided to evaluate the relative attenuation between the ten modes with the minimum ranked mode, TE₀₁. This evaluation is provided at three of the distances measured for the 1.07 m SDP. As noted in the table, within twelve meters the magnitude of the attenuation between the first rank and sixth rank mode is over two orders of magnitude. At $d_7 = 28.5$ m, the TE₀₁ mode's attenuation is at least 1/50 the other modes and is the dominant mode in governing the received power at sufficiently large distances. Based on these results, the approach followed in selecting the modes used for deriving the MBM is to use the M modes with the smallest attenuation coefficient. For the 1.07 m SDP study, this corresponds to the first seven modes in Table 2. Using the number of modes consistent with the number of measurements assists in numerical stability in optimizing the objective function. As illustrated in Table 2, M needs to be sufficiently large to incorporate the dominant modes contributing to defining the ellipsoid over the range of the data measurements.

Table 2. Modal attenuation coefficients for 1.07 m SDP with $R_s/\eta = 0.8$ and relative attenuation at d_i .

Rank	Mode	α_n (dB/m)	Relative Attenuation $(\alpha_1 - \alpha_n)d_i$ (dB)		
			$d_1 = 3.6$ m	$d_3 = 12.0$ m	$d_7 = 28.5$ m
1	TE ₀₁	0.24	0	0	0
2	TE ₀₂	0.84	2.2	7.2	17.1
3	TE ₁₂	0.96	2.6	8.6	20.5
4	TE ₁₃	1.46	4.4	14.6	34.8
5	TE ₀₃	1.85	5.9	19.3	45.9
6	TE ₂₂	2.08	6.7	22.0	52.4
7	TE ₂₃	2.36	7.7	25.4	60.4
8	TE ₁₄	2.62	8.7	28.5	67.8
9	TE ₄₂	3.33	11.3	37.0	88.0
10	TE ₀₄	3.37	11.4	37.4	89.1

3.2.2. Sensitivity of MBM Solution to Variation in R_s/η

As illustrated previously, the attenuation coefficients, α_n , plays a pivotal role in deriving the MBM. From (3), the intrinsic impedance ratio R_s/η is required to evaluate α_n . The ratio varies between 0.7 for a good conductor to 1.0 for a perfect dielectric [15]. The intrinsic impedance ratio models the physical nature of the material used to construct the SDP. Research on electrical properties of concrete indicates that dry concrete can be an insulator or a semiconductor [19]. Its electrical conductivity is strongly influenced by the presence of local moisture content as well as the penetration of ionic content of chlorides through the surface pores [20]. These factors tend to increase the conductivity of concrete. Hence, it is reasonable to assume that the concrete SDPs having a thin layer of water with impurities (e.g., NaCl/other chlorides), as observed during our measurement campaign, are most likely to act as semiconductor with $0.7 < R_s/\eta < 1.0$. The values of α_n in Table 2 are evaluated using $R_s/\eta = 0.8$. To illustrate the intrinsic impedance ratio's impact, the TE₀₁ attenuation coefficient varies between 0.22 dB/m to 0.28 dB/m over $0.7 \leq R_s/\eta \leq 0.9$. Due to the uncertainty associated with the value of the intrinsic impedance ratio, the sensitivity of the MBM to variation in R_s/η is evaluated using the 1.07 m SDP data measurements. This sensitivity is assessed by evaluating α_n using $R_s/\eta = 0.7, 0.725, 0.75, \dots, 0.9$. These values of α_n are, in turn, used to determine $\{P_n\}^*$, using (6). As discussed in Section 3.2.1, the objective function was evaluated

Table 3. Estimated mode coupled powers over variation in the intrinsic impedance ratio for 1.07 m SDP.

R_s/η	P_1	P_2	P_3	P_4	P_5	P_6	P_7	RMS Error (dB)
0.7	-38.6	-99.5	-99.9	-29.8	-12.2	-87.7	-95.6	5.12
0.725	-38.7	-108.1	-83.9	-16.5	-17.4	-76.5	-79.2	5.14
0.75	-38.5	-97.9	-86.0	-14.7	-69.1	-109.3	-109.0	5.12
0.775	-38.2	-106.5	-76.7	-14.2	-60.3	-105.8	-108.0	5.11
0.8	-38.0	-107.9	-73.3	-13.7	-92.8	-94.6	-94.1	5.11
0.825	-37.7	-108.3	-79.5	-13.2	-75.2	-108.6	-102.7	5.12
0.85	-37.5	-94.4	-86.8	-12.7	-92.5	-105.6	-97.0	5.13
0.875	-37.2	-95.5	-98.3	-12.3	-109.4	-108.2	-109.0	5.16
0.9	-37.0	-84.2	-88.4	-11.8	-109.0	-109.0	-109.0	5.19

using the seven modes with the smallest attenuation coefficients. Additional details concerning the optimization procedure are presented in Section 3.2.3. Fig. 3 depicts the resulting graph of the RMS error versus R_s/η . As indicated in the figure, the minimum RMS error occurs at approximately $R_s/\eta = 0.8$. The results show the RMS error only varies slightly around the minimum. Table 3 provides $\{P_n\}^*$ for each of the R_s/η values evaluated. The values of $\{P_n\}^*$ remain consistent for perturbations of R_s/η around the minimum with significant deviation in the mode coupled power when the intrinsic impedance ratio approaches a good conductor. Fig. 4 depicts graphs of three MBM models based on $R_s/\eta = 0.7, 0.8, 0.9$. These results suggest small variations in R_s/η will have minimal impact on the derivation of the MBM for the SDP. In the remainder of the paper $R_s/\eta = 0.8$ is assumed.

3.2.3. Optimizing the MBM Mode Coupled Power

The optimization problem posed in (4) could be solved directly using linear least square optimization with non-negativity constraint in order to estimate $\{P_n\}^*$. The difficulty with this approach is the numerical instability caused by both the dynamic range for the values of C_{in} and P_n as suggested by the values in Tables 3 and 4. Based on this

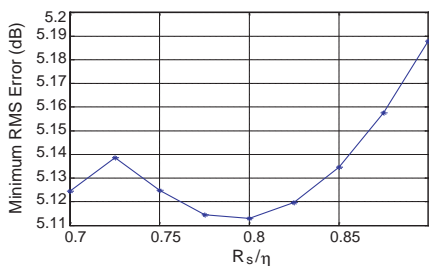


Figure 3. Sensitivity analysis of the MBM to the variation in the intrinsic impedance ratio.

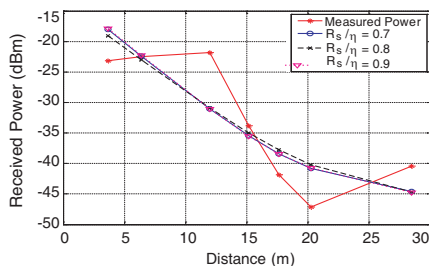


Figure 4. Received Power vs. distance with variation in R_s/η for 1.07 m SDP.

Table 4. Mode coupled powers illustrating variation in local optimal solutions (1.07 m SDP).

Solution Number	P_1	P_2	P_3	P_4	P_5	P_6	P_7	RMS Error (dB)	Distance (dB)
1	-38.0	-107.9	-73.3	-13.7	-92.8	-94.6	-94.1	5.11	-
2	-38.0	-108.7	-106.1	-13.7	-109.5	-109.5	-109.5	5.11	-80.2
3	-38.0	-108.0	-47.2	-13.7	-76.1	-91.0	-82.2	5.11	-71.7
4	-38.0	-56.1	-108.8	-13.7	-40.9	-98.0	-84.1	5.11	-67.4
5	-38.0	-106.9	-62.2	-13.7	-37.0	-91.8	-84.6	5.11	-63.7
6	-38.0	-107.5	-108.2	-13.7	-30.9	-57.3	-85.9	5.11	-57.6
7	-38.0	-108.7	-108.0	-13.7	-29.2	-92.2	-83.1	5.12	-55.9
8	-38.0	-107.2	-109.2	-13.9	-23.6	-90.3	-82.6	5.12	-50.3

observation, the optimization was formulated based on the logarithmic error. Using this formulation, a non-linear least square curve fitting optimization algorithm, *lsqcurvefit*, provided in Mathwork’s Matlab, was used to estimate the optimal mode coupled powers. The *lsqcurvefit* algorithm requires an initial estimate for $\{P_n\}$ from which it estimates the local optimal minimum $\{P_n\}_{Local}^*$. In order to enhance the likelihood of estimating the global minimum, a multi-start approach was employed where the initial $\{P_n\}$ was a permutation on a grid, i.e.,

$$\{P_n\}_j^* = lsqcurvefit \left(\{P_n\}_j \right) \quad (7)$$

where $P_n = \{-70, -60, \dots, -30\}$ dBm. Using (7), the corresponding RMS error for the local optimal solution $\{P_n\}_j^*$ is $\bar{\epsilon}_j$. The estimate for

the global optimal solution is then

$$\{P_n\}_{Global}^* = \arg \min_{\{P_n\}_j^*} \{\bar{\varepsilon}_j\}. \quad (8)$$

Table 4 provides eight examples of the local optimal solutions for the mode coupled powers. The first row in the table is an estimate of the global solution. The other examples were selected to illustrate variation in the local optimal solution and the solutions are rank ordered based on the minimum RMS error. The RMS error for each solution is given as well as the Euclidean distance between the global optimal solution $\{P_n\}_{Global}^*$ and the corresponding local optimal solution $\{P_n\}_j^*$. For consistency the indexing of the mode coupled power P_n in Table 4 is the same as the index of the corresponding attenuation coefficients and modes in Table 2.

From the results given in Table 4, the local optimal solution for the MBM varies from 2 to 4 dominant modes. Modes 1 and 4 (TE₀₁ and TE₁₃, respectively) remain dominant for all of the solutions, with variations in the relative importance of modes 2, 3 and 5. The histogram in Fig. 5 shows the distribution of the distance measures between the estimated global optimal solution and the local optimal solutions for all $\{P_n\}_j^*$ obtained over the multi-start grid. Distance locations annotated on the histogram correspond to solutions given in Table 4. The histogram suggests that the 2 mode solution (e.g., solutions 1 and 2) are common where as the 3 and 4 mode solutions are less common. In Fig. 6, a histogram of the normalized RMS Error $((\bar{\varepsilon}_{Global}/\bar{\varepsilon}_j) \times 100)$ evaluated over all local optimal solutions is given.

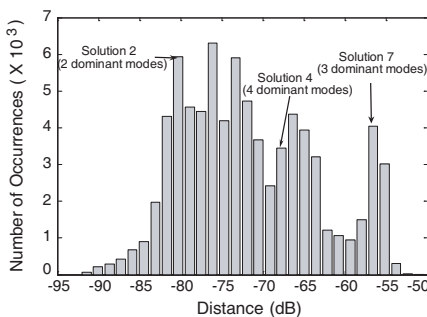


Figure 5. Histogram of Euclidean distance between $\{P_n\}_{Global}^*$ and $\{P_n\}_j^* \forall_j$ evaluated on the multi-start grid for 1.07 m SDP.

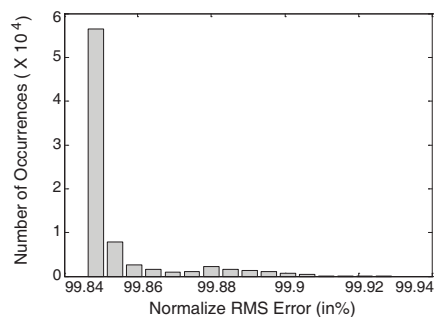


Figure 6. Histogram of the normalized RMS Error $(\bar{\varepsilon}_{Global}/\bar{\varepsilon}_j) \times 100 \forall_j$ evaluated on the multi-start grid for 1.07 m diameter SDP.

The variation in the RMS error between the local optimal solutions and global solution is essentially insignificant. From this, it is inferred that even if the solution for $\{P_n\}_j^*$ has distinct differences, as indicated by the results in Table 4, the RMS error between the measured data and the MBM models is consistent at approximately 5.11 dB.

3.2.4. Comparison of MBM with a Log Linear Model

In Fig. 7, models of the received power versus distance are graphed based on MBMs' derived for the 0.76 m and 1.07 m SDPs. The derivation of the MBM for the 0.76 m SDP followed the same procedure as outlined in the paper for the 1.07 m SDP, using the five empirical data points in Fig. 1. The estimates for optimal parameters for the 0.76 m SDP MBM are given in Table 5.

For comparison purposes, log-linear models [12] based on the 0.76 m and 1.07 m SDP empirical data sets are graphed in Fig. 7. The log-linear model minimizes the MSE between the data points and a linear model where the received power is expressed in dB. The MBM predicted coverage distance, given 110 dB dynamic range,

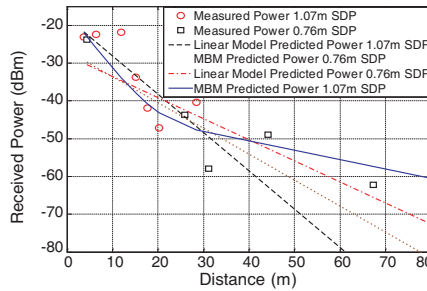


Figure 7. Comparison of the received power MBM models and the log linear models for 1.07 m and 0.76 m SDPs.

Table 5. Mode based model parameters for 0.76 m SDP.

Mode	n	P_n (dBm)	α_n (dBm)
TE ₀₁	1	-23.7	0.7
TE ₁₂	2	-42.0	2.0
TE ₀₂	3	-45.6	2.4
TE ₁₃	4	-54.6	3.9
TE ₂₂	5	-70.4	4.0

is approximately 110 m and 240 m for the 0.76 m and 1.07 m SDPs, respectively. From the graph in Fig. 7, it is evident that the empirical data sets are inadequate for estimating the received power characteristics over the desired dynamic range. The log-linear model is highly influenced by the distribution of the limited data set. As an example, for the 1.07 m SDP, the measurements are clustered at relatively short distances; hence, the log-linear model captures the effect of the modes with higher attenuation coefficients. The log-linear models provide poor estimates over the desired coverage distance due to the need to extrapolate the solution beyond the range of the limited data sets. The MBM does not have the same limitation since the data set is not used directly to fit the graph to the data points.

4. CONCLUSION

The MBM approach to characterize RF propagation within underground conduits is developed. The motivation for this work is derived from WSN application for condition based monitoring within conduits using typical wireless transceivers operating in the 2.4 GHz ISM band. The modeling approach is general and can be applied to conduits with varying diameters and different wall materials. The model addresses the difficulty associated with collecting empirical data from underground conduits and the requirement for obtaining a data set which covers the wireless transceiver's dynamic range. Unlike log-linear modeling approach, the minimum number of data points required for the MBM is governed by the number of dominant modes. Based on the SDP analysis, the number of dominant modes over the operational range of interest is less than five. In addition, the MBM requires estimating R_s/η that depends on physical properties of conduit walls. It is shown for the SDPs that the MBM is not sensitive to the uncertainty associated with estimating R_s/η . We conclude, from our findings that the MBM approach provides a more reliable method for estimating the received power as compared to the log-linear model. This is especially evident when the model is required to estimate received power outside the range of the empirical data set.

ACKNOWLEDGMENT

This work was supported by the Charlotte Mecklenburg Utilities Department (CMUD) under grant 555991 and in part by a subcontract from InfoSense, Inc through NSF SBIR award number IIP-0912589. The authors thank both the sponsors. Special thanks are also due to CMUD for their support during the measurement campaign.

REFERENCES

1. Emslie, A., R. Lagace, and P. Strong, "Theory of the propagation of UHF radio waves in coal mine tunnels," *IEEE Trans. Antennas Propag.*, Vol. 23, No. 2, 192–205, Mar. 1975.
2. Didascalou, D., J. Maurer, and W. Wiesbeck, "Subway tunnel guided electromagnetic wave propagation at mobile communication frequencies," *IEEE Trans. Antennas Propag.*, Vol. 49, No. 11, 1590–1596, Nov. 2001.
3. Lienard, M. and P. Degauque, "Natural wave propagation in mine environments," *IEEE Trans. Antennas Propag.*, Vol. 48, No. 9, 1326–1339, Sep. 2000.
4. Nikitin, P., D. D. Stancil, O. K. Tonguz, A. Cepni, A. Xhafa, and D. Brodtkorb, "Propagation model for the HVAC duct as a communication channel," *IEEE Trans. Antennas Propag.*, Vol. 51, No. 5, 945–951, May 2003.
5. Nikitin, P., D. Stancil, A. Cepni, A. Xhafa, O. Tonguz, and D. Brodtkorb, "A novel mode content analysis technique for antennas in multimode waveguides," *IEEE Trans. Microw. Theory Tech.*, Vol. 51, No. 12, 2402–2408, Dec. 2003.
6. Zhi, S. and I. F. Akyildiz, "Channel modeling of wireless networks in tunnels," *IEEE Global Telecommunications Conference (GLOBECOM'08)*, New Orleans, LA, Nov. 30–Dec. 4, 2008.
7. Martelly, R. and R. Janaswamy, "An ADI-PE approach for modeling radio transmission loss in tunnels," *IEEE Trans. Antennas Propag.*, Vol. 57, No. 6, 1759–1770, Jun. 2009.
8. Kim, J., J. Lim, J. Friedman, U. Lee, L. Vieira, D. Rosso, M. Gerla, and M. Srivastava, "SewerSnort: A drifting sensor for in-situ sewer gas monitoring," *Sixth Annual IEEE Communications Society Conference on Sensor, Mesh and Ad Hoc Communications and Networks (SECON 2009)*, Rome, Italy, Jun. 2009.
9. DeHaan, J. and M. Jacobs, "Tunnel communication test results," *Hydroelectric Research and Technical Services Group*, Bureau of Reclamation, U.S. Dept. of Interior, Sep. 1998.
10. Kjeldsen, E. and M. Hopkins, "An experimental look at RF propagation in narrow tunnels," *Proc. IEEE Military Communications Conf. (MILCOM'06)*, Washington D.C., Oct. 23–25, 2006.
11. Howitt, I., "Monitoring systems and methods for sewer and other conduit systems," US Patent Pending 12/399,492.
12. Rappaport, T. S., *Wireless Communications: Principles and Practice*. Prentice Hall, Englewood Cliffs, NJ, 1996.

13. Bertoni, H. L., *Radio Propagation for Modern Wireless Systems*, Prentice Hall, Englewood Cliffs, NJ, 2000.
14. Howitt, I. L., M. S. Khan, and J. S. Khan, "A mode based model for radio wave propagation in storm drain pipes," *PIERS Online*, Vol. 4, No. 6, 635–640, Jul. 2008.
15. Harrington, R. F., *Time Harmonic Electromagnetic Fields*, McGraw-Hill, 1961.
16. Howitt, I., S. Khan, and J. Khan, "Lumped parameter radio wave propagation model for storm drain pipes," *Proceedings of First International Conference on Computer, Control and Communications*, Karachi, Pakistan, Nov. 12–13, 2007.
17. Khan, J., "Radio frequency propagation study in storm drain pipes," UNCC ECE Department MS Thesis, 2007.
18. Boyd, S. and L. Vandenberghe, *Convex Optimization*, Cambridge University Press, 2004.
19. Shi, C., "Effect of mixing proportions of concrete on its electrical conductivity and the rapid chloride permeability test (ASTM C1202 or ASSHTO T277) results," *Cement and Concrete Research*, Vol. 34, 537–545, 2004.
20. Rajabipour, F., J. Weiss, and D. Abraham, "Insitu electrical conductivity measurements to assess moisture and ionic transport in concrete (a discussion of critical features that influence the measurements), Online report available at http://cobweb.ecn.purdue.edu/~concrete/weiss/publications/o_conference/OC-021.pdf.